Received: 13 November 2020 | Revised: 26 May 2021 | Accepted: 3 June 2021

DOI: 10.1002/we.2663

RESEARCH ARTICLE

WILEY

Wind turbine robust disturbance accommodating control using non-smooth H_∞ optimization

M. Hung Do[1,2] | Dirk Söffker[1]

[1]Chair of Dynamics and Control, University of Duisburg-Essen, Duisburg, Germany

[2]Department of Automation and Control of Thermal Processes, Hanoi University of Science and Technology, Hanoi, Vietnam

Correspondence
M. Hung Do, Chair of Dynamics and Control, University of Duisburg-Essen, Lotharstr. 1, Duisburg, 47057, Germany.
Email: hung.do@uni-due.de

Funding information
Vietnam International Education Development (VIED) scholarship

Summary

Disturbance accommodating control (DAC) has been developed in the last decades for wind turbines to control the rotor/generator speed and to reduce structural loads. The method allows accommodating unknown disturbance effects by using the combination of disturbance observers and disturbance rejection controllers. The actual main problem of DAC is to define suitable disturbance observer and controller gain matrices to achieve the desired overall performance including turbine speed regulation in combination with structural load mitigation. The disturbance rejection controller is often designed and tuned separately for individual applications and operating conditions. The closed-loop system stability and uncertainties due to the use of the linearized reduced-order model in controller synthesis procedure are not fully considered. This paper introduces a method to design DAC by optimizing the observer and controller parameters simultaneously to guarantee system performance respecting to structural loads mitigation, power regulation, and robustness. To eliminate the rotor speed control steady-state error due to model uncertainties, partial integral action is included. Simulation results using NREL reference wind turbine models show that the proposed method successfully regulates the rotor speed without error despite the presence of the model uncertainties. Structural loads are also reduced using proposed method compared to DAC designed by Kronecker product method. The proposed approach is able to define a stable and robust DAC controller by solving a non-smooth H_∞ optimization problem with structure and stability constraints.

KEYWORDS
disturbance accommodating control, load mitigation, robust control, wind turbine

1 | INTRODUCTION

Structural load reduction and speed regulation are the main goals of large-scale wind turbines control in the above-rated region (wind speed region 3). In this region, the rotor speed or generator power needs to be regulated to the rated value guaranteeing system safety because the wind energy is surpassing the turbine capacity. Rotor speed is regulated by adjusting the blade pitch angles collectively or individually.[1]

Structural load mitigation is important to be considered because of the wind turbine size growth as a development in the last decade induced by economic factors. Multi-objective advanced control methods are needed to alleviate the load while maintaining the rotor speed at rated value. Related control approaches need to be robust and able to reduce the effects of unknown variable wind speed disturbances and modeling errors.

Disturbance accommodating control (DAC)[2] is an effective and widely applied technique to accommodate the effects of wind disturbance on the wind turbines.[3] The method introduces an additional feed-forward controller to compensate effects of changing wind speed and unknown disturbances in combination with a regular feedback controller. Often a predefined disturbance model is used in combination with general state-space system model to estimate the unknown inputs by an extended observer. The gain matrix of the disturbance observer needs to be designed carefully because of the trade-off between the error of disturbance estimation and the error caused by the model uncertainties. High observer gains are required to achieve good disturbance/state estimation; however, it also makes the observer more sensitive to measurement noise and unmodeled dynamics.[4] In addition, it is a challenge to define a suitable feed-forward disturbance rejection control gain matrix to guarantee system stability and totally cancel the disturbance effects.

In literature, disturbance observers are often designed using an extended system model and classical design methods such as pole placement[5,6] or Linear Quadratic Regulator (LQR).[7] However, tuning methods for a precise disturbance estimation and about effects of uncertainties on the estimation quality depending on the dynamics of the disturbances are not discussed.

The disturbance rejection controller is typically considered as feed-forward and is calculated separately. The feed-forward gain matrix can be found by using Moore-Penrose Pseudoinverse.[7] This method does not guarantee to find a nonzero matrix, especially with the presence of the actuator dynamics. The disturbance effects are not totally canceled by using this method leading to the steady-state error. In Wang et al.,[8,9] the Kronecker product is used to find the disturbance rejection gain matrix which completely cancels out the effects of disturbances; however, the steady-state error still exists due to the error in the disturbance estimation caused by the incorrect assumed wind disturbance model. Instead of calculating the disturbance rejection gain matrix individually, in Njiri and Söffker,[10] the feedback and feed-forward gain matrices are calculated simultaneously by using the extended system model including the disturbance model for the LQR synthesis procedure. The method considers the overall system stability; however, an assumption about the connection between unknown input and system states is needed to guarantee the exosystem controllability. In Do et al,[11] an extra integral loop is used in combination with the DAC to eliminate the rotor speed regulation steady-state error with the presence of the model uncertainties.

Most of the DAC design methods compute the disturbance observer, the feedback, and the disturbance controller gain matrices separately. The effects of state and disturbance estimation quality, system robustness, and overall system optimality are not fully considered. This paper develops a robust scheme for designing the DAC for wind turbines. Unlike previous works, the disturbance observer, feedback, and disturbance rejection gain matrices are optimized simultaneously using the H_∞ norm of the closed-loop generalized system. A partial integral action is included in the design process to eliminate the rotor speed control steady-state error due to the model uncertainties. The closed-loop stability is ensured by providing H_∞ norm constraint to the closed-loop transfer function matrix. The paper uses non-smooth H_∞ optimization with constraints[12] applied for wind turbines in a previous work.[13] In the previous work, the approach is applied for defining a traditional observer-based controller. In this work, additional disturbance observer and disturbance rejection controller are considered and calculated to accommodate the effects of varying wind speed. The proposed method successfully reduces the structural load (tower bending moment) and regulates the rotor speed without steady-state error despite the presence of the model uncertainties. The approach also is robust with respect to model errors caused by the use of simplified models.

The H_∞ approach was applied and field-tested for multi-objective robust control of wind turbines.[14-16] This contribution implies the similar idea of minimizing weighted H_∞ norms of system closed-loop transfer functions to achieve performance and robustness. However, the proposed controller is restricted using the DAC structure instead of a high-order H_∞ controller. In other words, DAC controller parameters are optimized using structured H_∞ approach[12] to improve disturbance accommodation and to show robustness advantages.

The contribution is structured as follows. The properties of the wind turbine model and simulation tool used are introduced in Section 2. Section 3 provides an overview of DAC approaches. The proposed robust DAC design approach based on H_∞ optimization is given in Section 4. The developed method is applied to control a wind turbine in the above-rated region. In Section 5, the simulation results of the proposed method and the DAC design method based on the Kronecker product are compared. Lastly, conclusions are outlined.

2 | WIND TURBINE MODEL DESCRIPTION

This contribution uses the FAST simulation tool[17] for evaluation and comparison of the proposed method. As an example, the proposed controller is designed and simulated for a WindPACT 1.5 MW onshore reference wind turbine[18] that is developed based on an actual commercial wind turbine. The simulation tool and wind turbine model used are identical to those in our published papers.[13,19]

The FAST tool provides a numerical process to obtain linearized models for controller design.[17] The tool computes the state-space system matrices for different azimuth positions of a predefined operating point. The state-space matrices are azimuth-averaged to obtain the final model for designing controllers. Typically, a reduced-order model is obtained because only several interested DOFs are enabled during the linearization process. In this contribution, the tower, blade, drive-train, and generator DOFs are used to obtain a linearized reduced-order model for designing the controller; however, all DOFs are enabled during the simulation step. The above-rated region (operation wind speed from 12 to 25 m/s) is considered so that the turbine model is linearized at 18 m/s hub-height wind speed with 20.463 rpm nominal rotor speed.

The state-space linearized reduced-order model is represented in a suitable coordinate as

$$\begin{aligned} \dot{x} &= Ax + Bu + B_d d, \\ y &= Cx, \end{aligned} \tag{1}$$

where $x \in \mathbb{R}^{11x1}$ denotes the mechanical state vector, $A \in \mathbb{R}^{11x11}$ the linearized system matrix, $B \in \mathbb{R}^{11x1}$ denotes the control input matrix, $B_d \in \mathbb{R}^{11x1}$ the disturbance matrix, and $C \in \mathbb{R}^{2x11}$ denotes the output matrix. The measured output $y \in \mathbb{R}^{2x1}$ includes rotor speed ω calculated from the generator speed through gearbox ratio and tower fore-aft bending moment ζ reflecting tower displacement. The control input $u \in \mathbb{R}^{1x1}$ denotes the perturbed collective blade pitch angle $\Delta\beta$, and the disturbance $d \in \mathbb{R}^{1x1}$ denotes the perturbed hub-height wind speed Δv. All variables are initialized at zero.

The detailed corresponding state vector is

$$x = \begin{bmatrix} \text{tower displacement (fore-aft)} \\ \text{drivetrain torsional displacement} \\ \text{blade 1 displacement (flap-wise)} \\ \text{blade 2 displacement (flap-wise)} \\ \text{blade 3 displacement (flap-wise)} \\ \text{generator speed} \\ \text{tower velocity} \\ \text{drivetrain torsional velocity} \\ \text{blade 1 velocity} \\ \text{blade 2 velocity} \\ \text{blade 3 velocity} \end{bmatrix}. \tag{2}$$

To compensate the effects of actuator dynamics, an additional actuator model is required because pitch actuator dynamics are not included in the FAST linearized model. For simplicity, a first-order lag (PT1) model is used to represent the actuator dynamics as

$$\beta = \frac{1}{s\tau_a + 1} u, \tag{3}$$

where β denotes the actual pitch angle, τ_a the actuator lag time, and u represents the desired pitch angle. The state-space actuator model is expressed as

$$\dot{\beta} = -1/\tau_a \beta + 1/\tau_a u. \tag{4}$$

From (1) and (4), the linear wind turbine model considering actuator dynamics is obtained as

$$\begin{aligned} \begin{bmatrix} \dot{x} \\ \dot{\beta} \end{bmatrix} &= \underbrace{\begin{bmatrix} A & B \\ 0 & -1/\tau_a \end{bmatrix}}_{A_a} \underbrace{\begin{bmatrix} x \\ \beta \end{bmatrix}}_{x_a} + \underbrace{\begin{bmatrix} 0 \\ 1/\tau_a \end{bmatrix}}_{B_a} u + \underbrace{\begin{bmatrix} B_d \\ 0 \end{bmatrix}}_{B_{da}} d \\ y &= \underbrace{\begin{bmatrix} C & 0 \end{bmatrix}}_{C_a} \begin{bmatrix} x \\ \beta \end{bmatrix}. \end{aligned} \tag{5}$$

3 | DISTURBANCE ACCOMMODATING CONTROL

This section provides a review of DAC design methods for the wind turbine application. Open problems and limitations of the existing approaches are also discussed.

In DAC theory, an assumed disturbances model is used to estimate the external disturbance.[2] For wind turbine applications, the varying wind speed affecting the blades is considered as the disturbance. The disturbance model is expressed as

$$\begin{aligned} \dot{x}_d &= Dx_d, \\ d &= Hx_d, \end{aligned} \tag{6}$$

with x_d denotes the disturbance state and D and H denote the disturbance state-space model. For stepwise constant uniform wind speed, they can be chosen as $D=0$, $H=1$.[20] In the general case that the wind dynamical behavior is unknown, the choice $D=0$ in combination with suitable observer gains can reconstruct arbitrary bounded dynamics.[21]

Combining (5) and (6), an expanded system can be obtained as

$$\begin{aligned}\begin{bmatrix}\dot{x}_a\\ \dot{x}_d\end{bmatrix} &= \underbrace{\begin{bmatrix}A_a & B_{da}H\\ 0 & D\end{bmatrix}}_{A_e}\underbrace{\begin{bmatrix}x_a\\ x_d\end{bmatrix}}_{x_e}+\underbrace{\begin{bmatrix}B_a\\ 0\end{bmatrix}}_{B_e}u,\\ y &= \underbrace{\begin{bmatrix}C_a & 0\end{bmatrix}}_{C_e}\begin{bmatrix}x_a\\ x_d\end{bmatrix}.\end{aligned} \tag{7}$$

System and disturbance states are estimated using a standard observer with the extended model

$$\begin{aligned}\begin{bmatrix}\dot{\hat{x}}_a\\ \dot{\hat{x}}_d\end{bmatrix} &= \begin{bmatrix}A_a & B_{da}H\\ 0 & D\end{bmatrix}\begin{bmatrix}\hat{x}_a\\ \hat{x}_d\end{bmatrix}+\begin{bmatrix}B_a\\ 0\end{bmatrix}u+L(y-\hat{y}),\\ \hat{y} &= \begin{bmatrix}C_a & 0\end{bmatrix}\begin{bmatrix}\hat{x}_a\\ \hat{x}_d\end{bmatrix}.\end{aligned} \tag{8}$$

The error e between the real and estimated states is expressed as

$$e=\begin{bmatrix}x_a-\hat{x}_a\\ x_d-\hat{x}_d\end{bmatrix}, \tag{9}$$

with the corresponding dynamic

$$\dot{e}=(A_e-LC_e)e. \tag{10}$$

Assuming (A_e, C_e) as observable, the matrix L (observer gain) can be determined by pole placement or LQR technique using the extended model (7) to make (10) stable, so the estimated error e converges to zero.

The estimated values are used to calculate the control variable

$$u=u_x+u_d=K_x\hat{x}_a+K_d\hat{x}_d, \tag{11}$$

where u_x realizes control objectives such as speed regulation and structural load mitigation and u_d mitigates the wind disturbance d effects (Figure 1). Assuming (A_a, B_a) as controllable, the feedback controller gain matrix K_x can be defined via standard state feedback control design techniques like LQR as

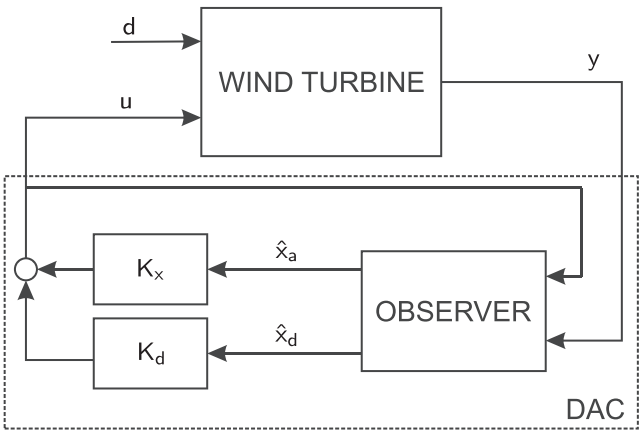

FIGURE 1 Disturbance accommodating control

$$K_x = R^{-1}B_a^T P, \tag{12}$$

with P is calculated using the Riccati equation

$$A_a P + P A_a^T + Q - P B_a R^{-1} B_a^T P = 0; \tag{13}$$

here, Q and R are positive definite. The matrices R and Q are designed to get the desired system dynamic responses.

The disturbance rejection controller gain matrix K_d is calculated separately to accommodate the effects of the unknown inputs. The closed-loop system with the controller can be expressed as

$$\begin{aligned} \dot{x}_a &= (A_a + B_a K_x)x_a + (B_a K_d + B_{da}H)x_d, \\ y &= C_a x_a. \end{aligned} \tag{14}$$

To accommodate the effects of the disturbance on the system dynamic, K_d is designed to minimize the norm $\|B_a K_d + B_{da}H\|$. The disturbance rejection controller gain matrix K_d can be calculated using Moore-Penrose Pseudoinverse ($\dagger$) as

$$K_d = -B_a^{\dagger} B_{da} H = -(B_a^T B_a)^{-1} B_a^T B_{da} H. \tag{15}$$

Generally, the norm $\|B_a K_d + B_{da}H\|$ is not equal to zero using K_d calculated from (15); thus, the effects of disturbances are not completely cancel. In addition, when use the actuator dynamics is considered, Equation 15 cannot provide nonzero gain matrix of the disturbance rejection controller.[7,9]

The Kronecker product method described in Wang et al[9] can be used to find a nonzero disturbance rejection controller K_d that, under given conditions, totally cancels the disturbance effects. The method calculates the disturbance rejection gain matrix K_d by solving the regulation equation as

$$\underbrace{\begin{bmatrix} A_a & B_a \\ C_a & 0 \end{bmatrix}}_{F} \begin{bmatrix} S_1 \\ S_2 \end{bmatrix} - \begin{bmatrix} S_1 \\ 0 \end{bmatrix} D = -\underbrace{\begin{bmatrix} B_{da}H \\ 0 \end{bmatrix}}_{J}. \tag{16}$$

The solutions S_1 and S_2 of (16) can be found using the Kronecker product as

$$\begin{bmatrix} S_1 \\ S_2 \end{bmatrix} = (I \bigotimes F + D \bigotimes I)^{-1}(-J); \tag{17}$$

here, $\bigotimes$ denotes the Kronecker product of two matrices.

The disturbance rejection gain matrix K_d is computed as

$$K_d = S_2 - K_x S_1; \tag{18}$$

this controller guarantees zero steady-state error if the system and disturbance models are completely precise. The condition to find a nonzero K_d is defined as

$$-J \in col(I \bigotimes F + D \bigotimes I); \tag{19}$$

here, *col*() denotes the column span space of a matrix. If $(I \otimes F + D \otimes I)$ has full column rank, the solution is unique.[9]

The overall disturbance accommodating controller including the observer, feedback controller K_x, and disturbance rejection controller K_d can be considered as a dynamic controller (Figure 1). Replacing the control variable u from (11), (8) can be rewritten as

$$\begin{bmatrix} \dot{\hat{x}}_a \\ \dot{\hat{x}}_d \end{bmatrix} = \begin{bmatrix} A_a & B_{da}H \\ 0 & D \end{bmatrix} \begin{bmatrix} \hat{x}_a \\ \hat{x}_d \end{bmatrix} + \begin{bmatrix} B_a \\ 0 \end{bmatrix} [K_x \;\; K_d] \begin{bmatrix} \hat{x}_a \\ \hat{x}_d \end{bmatrix} - \underbrace{\begin{bmatrix} L_1 \\ L_2 \end{bmatrix}}_{L} [C_a \;\; 0] \begin{bmatrix} \hat{x}_a \\ \hat{x}_d \end{bmatrix} + Ly; \tag{20}$$

here, L_1 denotes the observer gain matrix for system states, L_2 observer gain matrix for disturbances.

The DAC dynamic controller defined by L, K_x, and K_d is described as

$$\begin{aligned}\begin{bmatrix}\dot{\hat{x}}_a\\ \dot{\hat{x}}_d\end{bmatrix} &= \begin{bmatrix}A_a + B_aK_x - L_1C_a & B_{da}H + B_aK_d\\ -L_2C_a & D\end{bmatrix}\begin{bmatrix}\hat{x}_a\\ \hat{x}_d\end{bmatrix} + Ly,\\ u &= [K_x \;\; K_d]\begin{bmatrix}\hat{x}_a\\ \hat{x}_d\end{bmatrix}.\end{aligned} \tag{21}$$

Existing approaches to design DAC have following problems and limitations:

- Observer gain (L), state controller gain (K_x), and disturbance rejection gain (K_d) are calculated separately, the effects of state and disturbance estimation quality, and overall system optimality is not fully considered.[9,11]
- Disturbance rejection controller K_d is designed as a feed-forward controller. System stability when adding the disturbance rejection controller is not fully considered.[7]
- Precise turbine and wind disturbance models are required. System robustness regarding inaccurate models is not considered.[6,7,9]

Existing all-in-one approaches with the combination of Proportional-Integral-Observer (PIO)[21,22] and output control[23] solve all problems mentioned before but are very sensitive to measurement uncertainties as well as noise. The observer and controller gains are designed separately; assumptions related to the connection between unknown inputs and system states are needed to guarantee the exosystem controllability.[11]

In the wind turbine applications, the disturbance model may not be accurate due to uncertainties and stochastic variation of wind disturbance. Also, the use of linearized reduced-order models leads to inaccurate turbine models, especially when the turbine operates outside the given operating conditions. So it is necessary to develop a method to define robust DAC for wind turbines with respect to model and measurement uncertainties.

4 | ROBUST DISTURBANCE ACCOMMODATING CONTROL

The DAC design methods described in Section 3 calculate the observer, state controller, and disturbance controller separately. The overall system stability, robustness, and optimality are not fully considered. This section proposes a novel scheme to simultaneously compute the robust disturbance accommodating control (RDAC) parameters (L, K_x, and K_d) off-line. The idea is using the mixed-sensitivity H_∞ norm of the closed-loop transfer function as the cost function to optimize the DAC parameters.

4.1 | Robust H_∞ control background

The general H_∞ problem can be defined as the task to find the optimal stable controller for a plant P minimizing the H_∞ norm $\|.\|_\infty$ of the closed-loop transfer function (G_{zd}) from unknown disturbance inputs d to the regulated outputs z as

$$R_{opt} = \underset{R \in \mathcal{R}}{argmin} \|G_{zd}(P,R)\|_\infty, \tag{22}$$

where R_{opt} designates the optimized controller and $\mathcal{R}$ a group of controllers stabilizing P (Figure 2). The optimized controller minimizes unknown disturbance inputs effects to the outputs improving the system robustness. Linear Matrix Inequality (LMI)[24] or Riccati Equations (AREs)[25] approaches are typically used to find the optimal H_∞ controller.

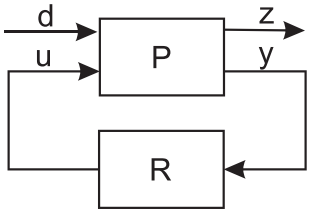

FIGURE 2 Standard H_∞ problem

There is a conflict between robustness against uncertainties and performances of the H_∞ approach.[26] The conflict can be solved by using weighting functions W_x for each regulated outputs (Figure 3); here, O denotes the transfer function of the original plant. The system dynamics at frequency ranges can be designed by choosing suitable weighting functions. The standard H_∞ optimization (22) is extended to the mixed-sensitivity loop shaping approach as

$$R_{opt} = \underset{R \in \mathcal{R}}{argmin} \left\| \begin{matrix} W_1 S \\ W_2 RS \\ W_3 T \end{matrix} \right\|_\infty . \tag{23}$$

By using additional weighting functions, the sensitivity function $S = (I + OR)^{-1}$ and other closed-loop transfer functions such as the complementary sensitivity function $T = I - S$ or RS can be designed to have the desired shapes. The transfer function RS maps unknown inputs d to the control inputs u. The gain of RS affects the bandwidth of the controller as well as the system robustness with respect to additive uncertainty. The complementary sensitivity T is the transfer function between the measurement noise or reference input to the output. The size of T is important for reference tracking, noise attenuation, and multiplicative uncertainty robustness.[26]

Typically, W_1 and W_3 are selected to have a small gain of S within the desired bandwidth to achieve good tracking control performance and to have a small T (large S) in the high-frequency range providing higher robustness against the multiplicative uncertainty. The weighting function W_2 can be a high-pass filter improving the stability margin with additive uncertainty and avoiding high-frequency control signal.

4.2 | Robust DAC approach

As presented in the previous section, the mixed-sensitivity H_∞ norm of the closed-loop transfer function is a good indicator for both system performance and robustness. The norm is used as the cost function to find the optimal robust DAC (RDAC). Unlike the standard H_∞ control finding the full-order controller, the proposed RDAC approach finds parameters of a "structured controller"[27] having the DAC structure (21). Non-smooth H_∞ synthesis proposed in Apkarian and Noll[28] is used to define the controller parameters with structural constraints. The similar approach was applied to find the robust observer-based controller in our previous paper.[13] In this contribution, as novelty, an additional disturbance observer and disturbance rejection controller are included to improve the disturbance accommodating performance.

The problem to find the robust disturbance accommodating controller (RDAC) is formulated as

$$RDAC = DAC_{opt} = \underset{DAC \in \mathcal{DAC}}{argmin} \|G_{zd}(P, DAC)\|_\infty, \tag{24}$$

where DAC denotes a controller having DAC structure (21), $\mathcal{DAC}$ a group of DAC controllers that stabilize P, and DAC_{opt} denotes the optimized controller defined by the optimal values of L, K_x, and K_d. With structural constraints, the problem (24) is non-convex and cannot be solved by traditional H_∞ approaches such as AREs or LMI.

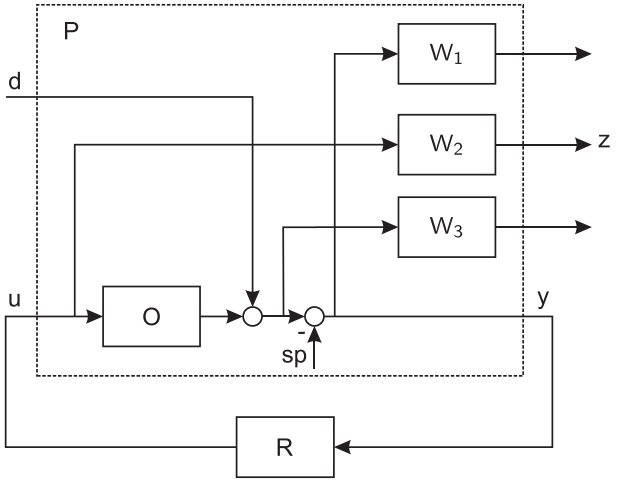

FIGURE 3 Mixed-sensitivity H_∞ control

To find a DAC controller stabilizing the closed-loop system, a stability constraint is added to the original optimization problem. Assuming full controllability and observability, a linear time-invariant system is Lyapunov stable if and only if the H_∞ norm of the closed-loop transfer function from inputs to outputs is finite,[29] so the stability constraint is fulfilled by

$$\|C_a(sI - \mathcal{A}(DAC))^{-1}B_a\|_\infty < +\infty, \tag{25}$$

where $\mathcal{A}(DAC)$ denotes the closed-loop system matrix depending on the controller *DAC*.

The task to define robust and optimal DAC controller is formulated as an optimization problem as

$$\begin{aligned} RDAC = DAC_{opt} = argmin \quad & \|G_{zd}(DAC)\|_\infty \\ s.t. \quad & \|C_a(sI - \mathcal{A}(DAC))^{-1}B_a\|_\infty < +\infty. \end{aligned} \tag{26}$$

The additional constraint (25) guarantees asymptotic stability of the controlled system when finding the optimal parameters for the DAC controller. Note that (26) must be initialized with a stabilizing controller. The H_∞ norms in (26) are calculated from the system closed-loop state-space model using a bisection algorithm.[30] The problem (26) is non-smooth and non-convex and can be solved using global optimization approaches such as Genetic Algorithm (GA).

By solving (26), the optimal parameters *L*, K_x, and K_d of the DAC controller are defined (Figure 4). A non-smooth optimization algorithm is proposed in Apkarian and Noll[28] to solve (26) with a reasonable balance between computing time and effectiveness. The Clarke sub-differential[31] and a multi-start steepest gradient descent method are used to find the optimal structured H_∞ controller. The stopping criterion is $\partial f(x) = 0$ indicating a critical point formulated as

$$inf\{\|g\| : g \in \partial f(x)\} < \epsilon; \tag{27}$$

here, ∂ denotes Clarke sub-differential, *f*(*x*) the cost function, and ϵ is a small positive number. When the criterion is fulfilled, it is assumed that a local optimum for defining *K*, *L* is defined. Due to the non-convex cost function, in general, it can be assumed that several local minima exist. The multi-start strategy is applied to overcome this problem. Finally, the best parameter set is applied. This heuristic approach solved practically the problem that the global optimum is unknown or the related search is too computationally costly. The detail optimization procedure can be found in Apkarian and Noll.[28]

The obtained RDAC controller is robust with respect to the minimization of mixed-sensitivity H_∞ norm of the closed-loop transfer function. The inaccuracies of system and disturbance models are considered as additive and multiplicative uncertainties. Suitable system performance and robustness can be achieved by designing the shape of weighting functions. With additional disturbance observer and disturbance rejection controller, the computed RDAC controller also can accommodate the effects of varying wind disturbance and can be realized as a standard DAC controller.

4.3 | Robust DAC for wind turbines

The proposed RDAC method is applied for wind turbine region 3 control (Figure 5). The *S*/*RS* mixed-sensitivity approach is used[26] shaping *S* and *RS* focusing on disturbance rejection, vibration damping, and robustness; the shape of *T* is reflected through the shape of *S*. The goals are to mitigate the structural load (here, for example, is the tower bending moment) and to regulate the rotor/generator speed at a predefined rated speed.

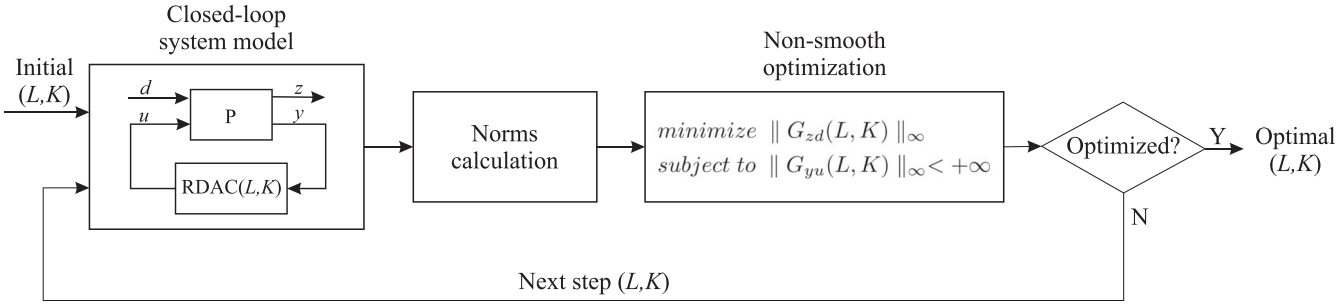

FIGURE 4 RDAC design using non-smooth H_∞ synthesis with constrains

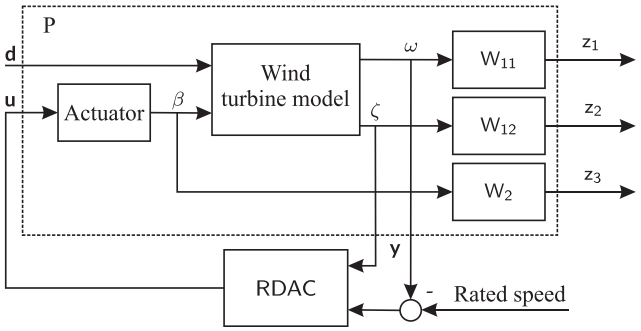

FIGURE 5 RDAC for wind turbines

The actuator is included in the plant P considering the blade pitch dynamics. Here, the control input is the collective blade pitch angle β, the wind speed d is considered as unknown disturbance, the measured outputs are the tower fore-aft bending moment ζ, and the rotor speed ω.

The generalized plant P of the wind turbine and actuator is expressed by

$$P: \begin{cases} \dot{x}_a = A_a x_a + B_a u + B_{da} d \\ y = C_a x_a \\ z = W C_z x_a; \end{cases} \tag{28}$$

here, W denotes the weighting function matrix and C_z the exogenous output matrix.

The desired robustness and performance are obtained by choosing the suitable weighting function matrix W. The exogenous output z with weighting functions are described as

$$\underbrace{\begin{bmatrix} z_1 \\ z_2 \\ z_3 \end{bmatrix}}_{z} = \underbrace{\begin{bmatrix} W_{11} & 0 & 0 \\ 0 & W_{12} & 0 \\ 0 & 0 & W_2 \end{bmatrix}}_{W} \begin{bmatrix} \omega \\ \zeta \\ \beta \end{bmatrix} = W C_z x_a. \tag{29}$$

For good speed regulation performance and robustness against wind disturbances, W_{11} is designed as a low-pass filter. The crossover frequency of the weighting function determines the bandwidth of the controller. Larger bandwidth provides faster responses and better control performance; however, the controller bandwidth is limited by the dynamics of the pitch actuator.[14] Also, high control bandwidth leads to less robustness, so a good balance of the value is required. The tower variation is reduced by choosing W_{12} as an inverted notch filter centered at the tower fore-aft frequency T_{fa} (6.55 rad/s) (Figure 6). To reduce high-frequency control activity, W_2 is selected as a high-pass filter. The designed weighting functions are given as

$$\begin{aligned} W_{11} &= \frac{0.045s + 0.125}{s + 0.025}, W_{12} = \frac{11.11s^2 + 11.11s + 72.82}{s^2 + 0.1s + 6.55}, \\ W_2 &= \frac{10s + 10}{0.01s + 1}. \end{aligned} \tag{30}$$

The weighting functions can be adapted to the desired objectives and actual wind dynamics for optimal situation-based operation.

To remove the rotor speed regulation steady-state tracking error, partial integral action is included in the RDAC controller. This can be realized by letting $S(0) = 0$ with some approximation to avoid numerical problems. In this contribution, the integral action is included directly in the controller. In this case, the order of the controller increases by one; however, it makes the balance between the performance of each output channel and robustness easier. The additional integral state x_i of the rotor speed measured output is introduced into the controller as

$$\begin{aligned} \dot{x}_i &= C_i y, \\ u &= K_x \hat{x}_a + K_d \hat{x}_d + K_i x_i, \end{aligned} \tag{31}$$

where the matrix C_i defines the location of the measured rotor speed in the outputs and K_i denotes the integral gain.

From (8) and (31), the DAC dynamic controller with partial integral action is described as

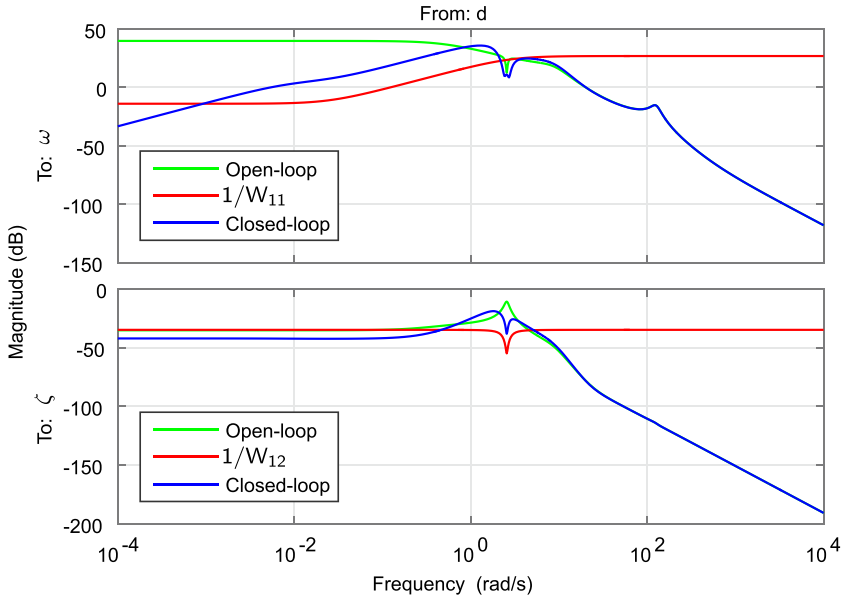

FIGURE 6 Bode plot of open-loop, inverted weighting functions, and closed-loop with RDAC [Colour figure can be viewed at wileyonlinelibrary.com]

$$\begin{bmatrix}\dot{\hat{x}}_a\\ \dot{\hat{x}}_d\\ \dot{x}_i\end{bmatrix} = \underbrace{\begin{bmatrix}A_a+B_aK_x-L_1C_a & B_{da}H+B_aK_d & B_aK_i\\ -L_2C_a & D & 0\\ 0 & 0 & 0\end{bmatrix}}_{A_r}\underbrace{\begin{bmatrix}\hat{x}_a\\ \hat{x}_d\\ x_i\end{bmatrix}}_{x_r} + \underbrace{\begin{bmatrix}L_1\\ L_2\\ C_i\end{bmatrix}}_{B_r} y,$$
$$u = \underbrace{\begin{bmatrix}K_x & K_d & K_i\end{bmatrix}}_{C_r}\begin{bmatrix}\hat{x}_a\\ \hat{x}_d\\ x_i\end{bmatrix}. \tag{32}$$

The DAC controller (32) is considered as a "structured controller."[27] The controller if defined by the parameter matrices K_x, K_d, K_i, and L.

$$DAC = DAC(L,K_x,K_d,K_i). \tag{33}$$

The condition for the existence of a DAC controller stabilizing P is the full controllability and observability of the extended system (7). The robust disturbance accommodating controller RDAC is defined by the optimal parameter matrices $K = [K_xK_dHK_i]$ and $L = [L_1L_2]^T$ obtained by solving the optimization problem (26) using non-smooth H_∞ synthesis.[28] To formulate the cost function and constraint in (26), the H_∞ norms of close-loop transfer functions need to be calculated.

The DAC controller (32) can be described as

$$DAC(L,K): \begin{cases}\dot{x}_r &= A_rx_r + B_ry\\ u &= C_rx_r;\end{cases} \tag{34}$$

here, $A_r(L, K)$, $B_r(L)$, and $C_r(K)$ as defined in (32).

Using (28) and (34), the closed-loop system is described as

$$\begin{bmatrix}\dot{x}_a\\ \dot{x}_r\\ y\\ z\end{bmatrix} = \begin{bmatrix}A_a & B_aC_r & B_{da}\\ B_rC_a & A_r & 0\\ C_a & 0 & 0\\ WC_z & 0 & 0\end{bmatrix}\begin{bmatrix}x_a\\ x_r\\ d\end{bmatrix}. \tag{35}$$

The behavior of closed-loop system (35) for a given weighting matrix W only depends on the controller matrices (A_r, B_r, C_r). The controller is based on the DAC structure (32) and determined by K and L gain matrices. Closed-loop transfer functions are derived from (35); the H_∞ norms of

the close-loop system then are calculated[30,32] to formulate the optimization problem (26). The optimal parameters K^* and L^* for the RDAC controller are obtained by solving (26) using the non-smooth H_∞ synthesis algorithm implemented in the MATLAB function hinfstruct.[12]

5 | RESULTS AND DISCUSSION

For validation of the proposed RDAC method, the FAST simulation software, developed by NREL, is used.[17] The controllers are designed using a linearized reduced-order model; however, the simulations are realized using a full-order nonlinear wind turbine model. This combination allows the representation of modeling errors due to the fact the controller is controlling the nonlinear system, but the design is based on the related linearized model. The control objectives are reducing the structural load (tower fore-aft bending moment) and regulating the rotor speed to a rated value of 20.463 rpm (rated generator speed 1,800 rpm). The standard load case for fatigue and normal power production is based on IEC 61400-1 DLC 1.2.[33] The proposed RDAC controller is evaluated and compared with a baseline DAC controller with two scenarios based on step and stochastic wind profiles. The state feedback and observer of the baseline DAC controller are designed by LQR techniques; the disturbance rejection controller is designed by Kronecker product method as described in Section 3. The DAC and RDAC controllers have the same order and structure (Equation 32); only parameters are different. Both controllers are designed using a single linearized wind turbine model at the wind speed of 18 m/s as given in Section 2. As mentioned in Wright,[34] the use of tower top acceleration (realistic measurement of modern turbines) measurement over tower bending moment/tower deflection shows no difference in DAC performance. With the development of strain measurement techniques (i.e., fiber optic strain gauge), the measurement of bending moment also becomes realistic and can represent directly the structural load. For the simplicity of system matrices, in this contribution, the tower bending moment measurement is used. Details of the controller/observer matrices ($L \in \mathbb{R}^{13x2}, K_x \in \mathbb{R}^{1x12}, K_d \in \mathbb{R}^{1x1}, K_i \in \mathbb{R}^{1x1}$) of DAC and RDAC are given in Table 1.

5.1 | Step wind profile results

For assessing the regulation performances and robustness of the proposed RDAC approach with changing operation point (wind speed), a step wind profile changing from 14 to 22 m/s is applied (Figure 7a). The model used for controller design is linearized at the wind speed of 18 m/s. When the turbine operates at the wind speed differ from the selected linearized point, the model is not precise due to the nonlinearity nature of wind turbines. In Figure 7b, the rotor speed responses of the RDAC approach and the baseline DAC solved via Kronecker Product (DAC) are shown. It can be observed that the baseline DAC approach cannot provide zero steady-state error due to the model mismatch caused by unmodeled dynamics and nonlinearities of the wind turbine. On the other hand, the proposed method successfully regulates the rotor speed to the rated speed without static error. Some low-frequency variations are introduced in the RDAC result due to the effect of integral action. The proposed RDAC approach has good regulation performance over a wide range of operation wind speed indicating high robustness with respect to wind speed variation.

TABLE 1 Gains of matrices ($L \in \mathbb{R}^{13x2}, K_x \in \mathbb{R}^{1x12}, K_d \in \mathbb{R}^{1x1}, K_i \in \mathbb{R}^{1x1}$) of DAC and RDAC

DAC					RDAC				
L		K_x^T	K_d^T	K_i^T	L		K_x^T	K_d^T	K_i^T
0.291	0.929	−229.976	2.518	0.001	−3.465	6.930	0.661	0.413	−0.002
0.000	0.000	−207.811			0.576	−1.841	−26.551		
1.490	0.390	−3.542			29.493	−57.091	−8.662		
1.490	0.390	−5.680			29.328	−57.380	4.727		
1.490	0.390	−5.679			27.444	−49.512	3.637		
−0.253	−0.026	−81.413			2.160	−9.007	−0.479		
0.317	0.000	−48.729			−0.036	−25.023	−2.396		
0.002	0.000	−35.676			3.449	22.432	0.524		
1.804	1.044	−0.442			−8.704	−61.538	1.237		
1.804	1.044	−0.680			−9.093	−68.707	−0.719		
1.804	1.044	−0.680			−31.844	−21.858	−0.595		
0.000	0.000	21.010			−0.136	−0.948	2.546		
9.782	2.076				0.180	−0.253			

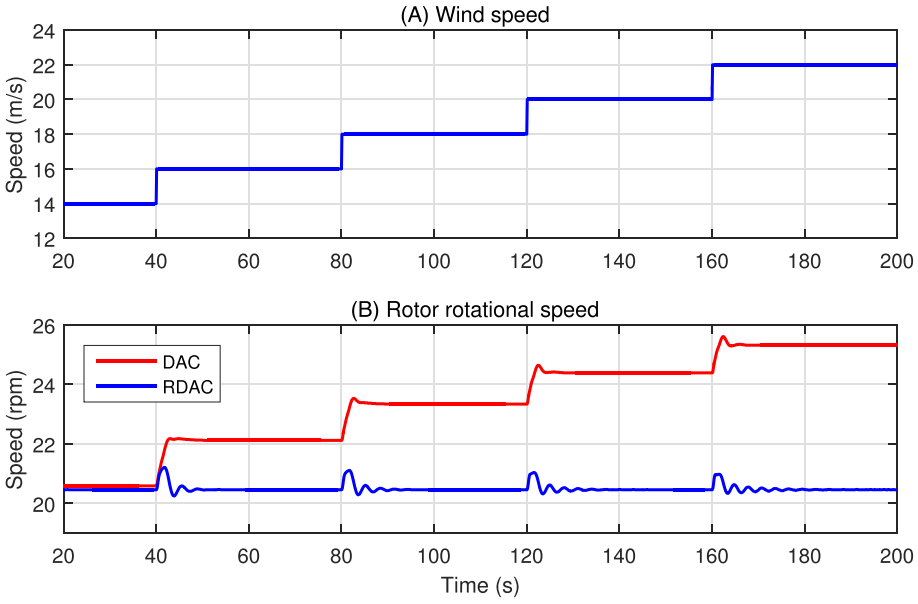

FIGURE 7 Responses of step wind profile [Colour figure can be viewed at wileyonlinelibrary.com]

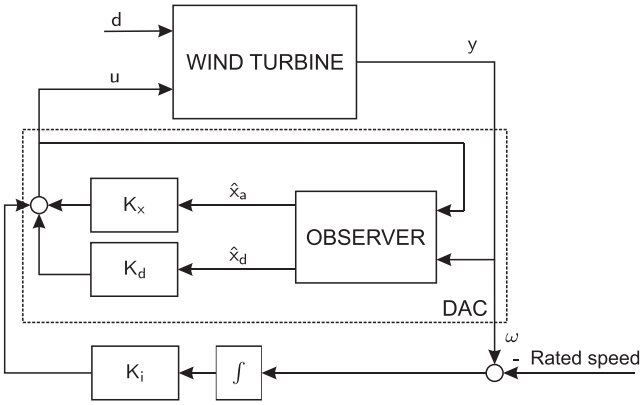

FIGURE 8 Disturbance accommodating control with integral action

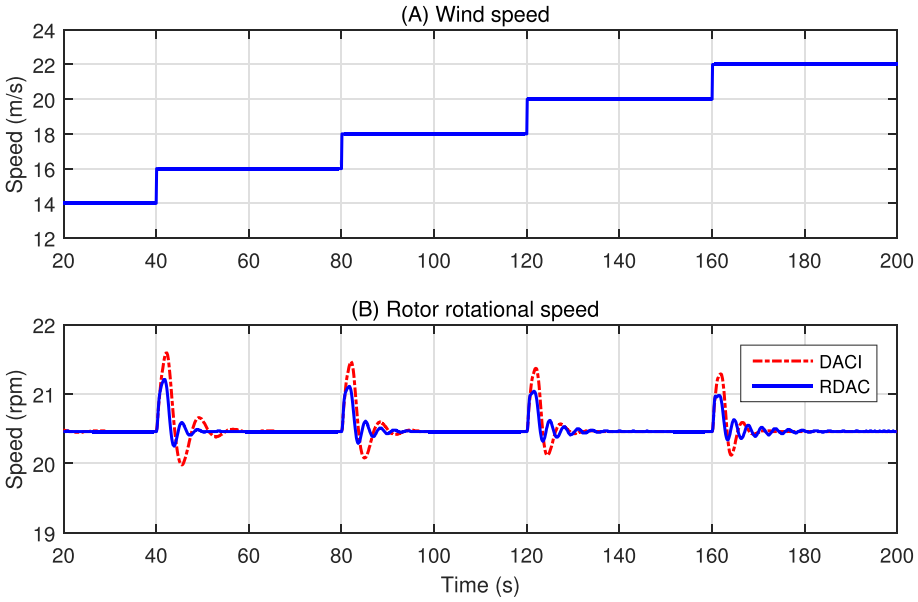

FIGURE 9 Responses of step wind profile—with integral action [Colour figure can be viewed at wileyonlinelibrary.com]

Gain-scheduled techniques can be used to handle the problem of changing operating points. However, the techniques often require wind speed information which typically is not available. Besides, it is difficult to determine the switching conditions for stochastic wind conditions resulting in complex controllers. There is no guarantee of stability and performance per se when controller parameters are interpolated between linearized operating points. In Dykes and Rinker,[18] a baseline gain-scheduled PI controller is presented using the pitch angle as scheduling variable. The approach only regulates the rotor speed without considering structural load. Comparisons between the gain-scheduled PI controller and the proposed RDAC approach that has fixed parameters were given in our previous paper.[13]

To eliminate the static error of the baseline DAC, an additional integral control loop of the rotor speed, which is required to be tuned separately, is used in combination with the baseline DAC (Figure 8). The results of DAC with integral action method (DACI) are compared to that of RDAC (Figure 9). Note that the proposed RDAC method also has the partial integral action (31), the integral gain K_i in this case is optimized with other parameters. The RDAC method provides lower settling time and over-shoot than that of the baseline DAC with the integral loop (DACI) indicating better speed regulation performance. The closed-loop singular values plot is shown in Figure 10. The maximum singular value is an important term to evaluate the performance and robustness of the system. For a MIMO system, the maximum singular value is equal to the largest system gain. A lower maximum singular value results in a less sensitive or more robust system in the worst scenario.[26] As shown in Figure 10, a reduction in maximum singular value (mapping from disturbance d to output y) is achieved using RDAC compared with the DACI approach.

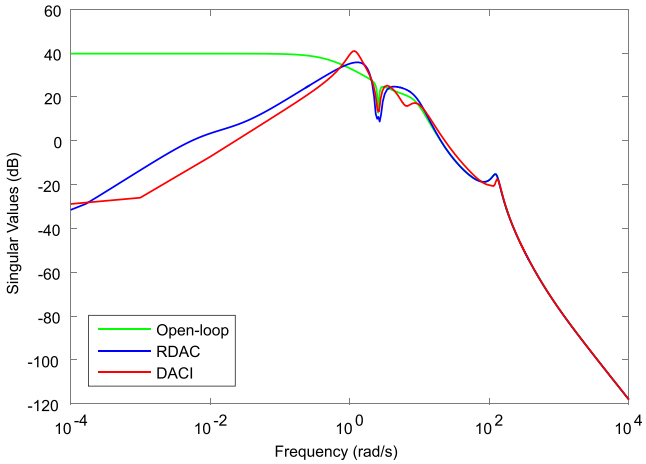

FIGURE 10 Singular values plot of open-loop and closed-loop systems from disturbance d to output y (DACI, DAC with integral action; RDAC, Robust DAC) [Colour figure can be viewed at wileyonlinelibrary.com]

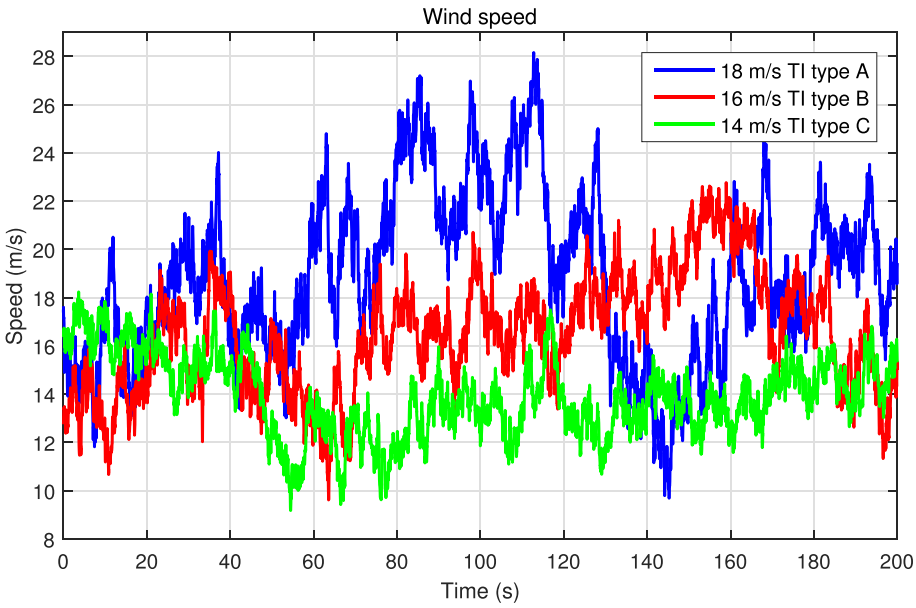

FIGURE 11 Stochastic wind profiles [Colour figure can be viewed at wileyonlinelibrary.com]

5.2 | Stochastic wind profile results

For more realistic working conditions and the investigation of wind disturbances rejection ability of the controllers (RDAC and DACI), stochastic wind profiles with different turbulence intensity (TI) level and mean wind speed are used (Figure 11). The wind profiles followed the IEC 61400-1 standard[33] and are generated using TurbSim[35] based on the von Karman wind turbulence model using different random seeds. The wind profiles

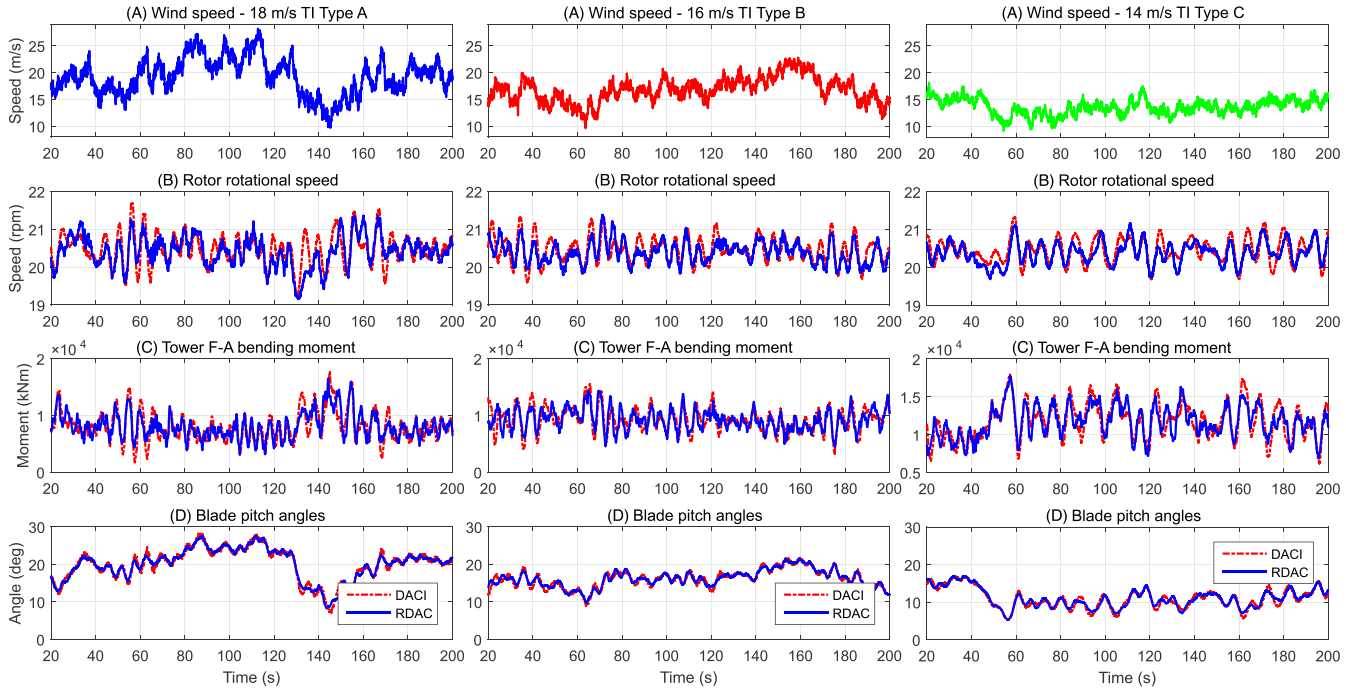

FIGURE 12 Responses of stochastic wind profile (DACI, DAC with integral action; RDAC, Robust DAC) [Colour figure can be viewed at wileyonlinelibrary.com]

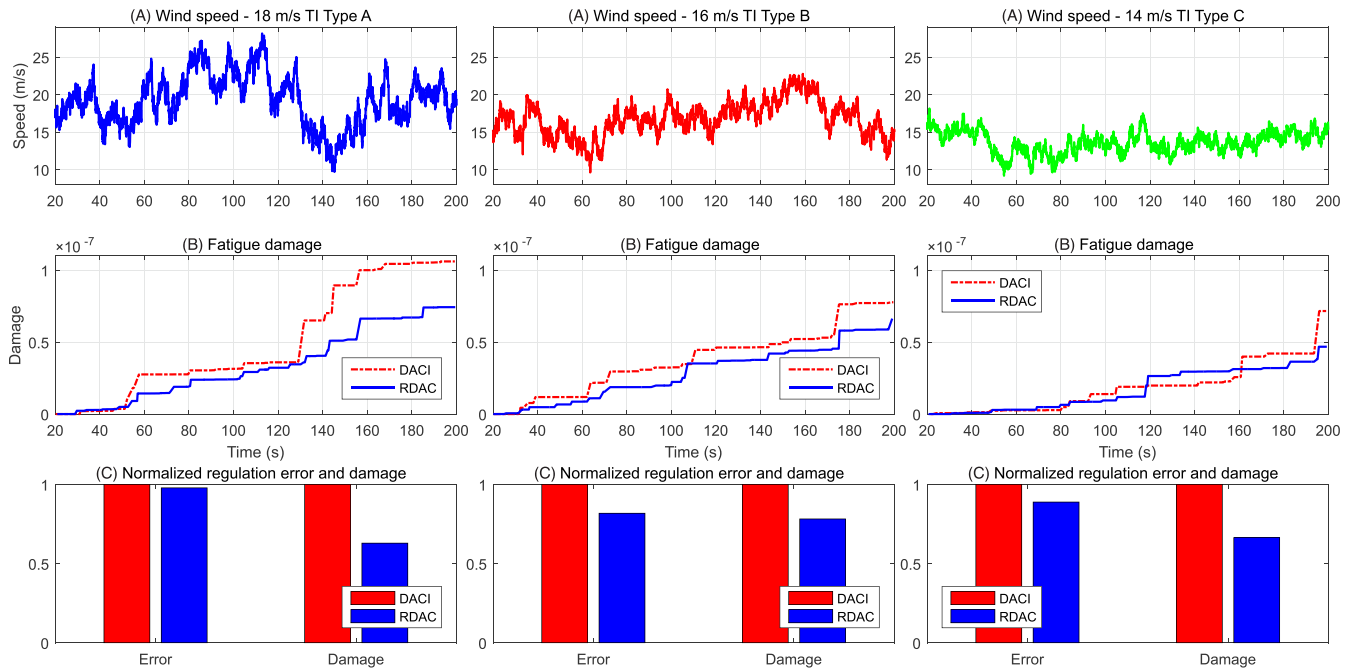

FIGURE 13 Regulation error and fatigue damage (DACI, DAC with integral action; RDAC, Robust DAC) [Colour figure can be viewed at wileyonlinelibrary.com]

are chosen to have the mean speed of 18, 16, and 14 m/s, and the turbulence level of A, B, and C, respectively. Here, turbulence level A is the most turbulence level regarding the IEC categories standard with the expected value of TI at 15 m/s is 16 %.[35]

In figure 12, the simulation results for stochastic wind are shown. The proposed RDAC method has lower speed variation for all considered wind profiles as observed from figure 12.b. This means the proposed controller provides better speed control performance than the DACI method. The tower load is also mitigated by using RDAC indicated by lower tower bending moment variation amplitude compare to that of the DACI controller (Figure 12c). The control variables (collective blade pitch angle) of two controllers are shown in Figure 12d.

Quantitative evaluation of the results is realized using the mean square rotor speed regulation error and the tower fatigue damage.[36] The cumulative fatigue damage of the tower is calculated from the tower bending moment time series using Miner's rule[37] and rainflow-counting

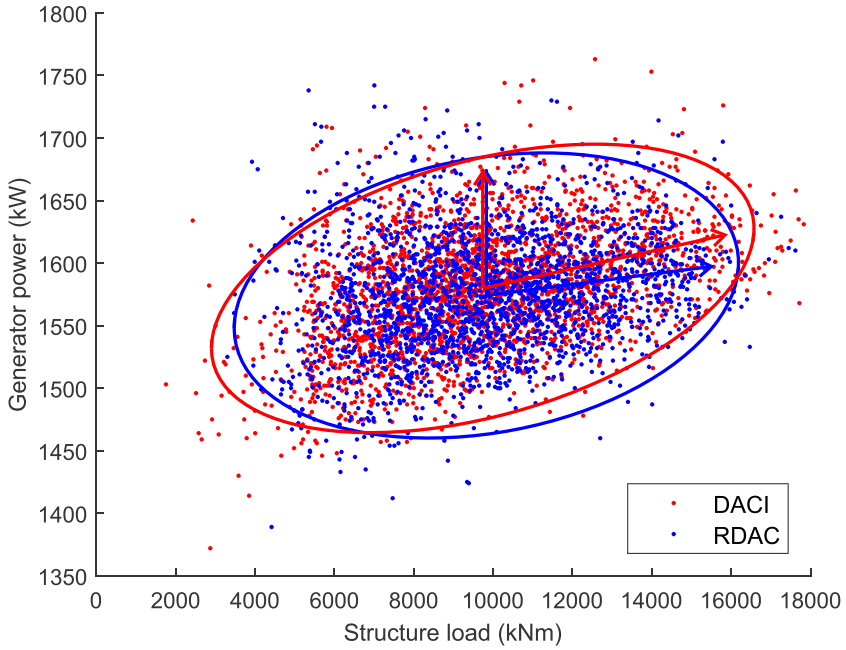

FIGURE 14 Power-load covariance distribution diagram (DACI, DAC with integral action; RDAC, Robust DAC) [Colour figure can be viewed at wileyonlinelibrary.com]

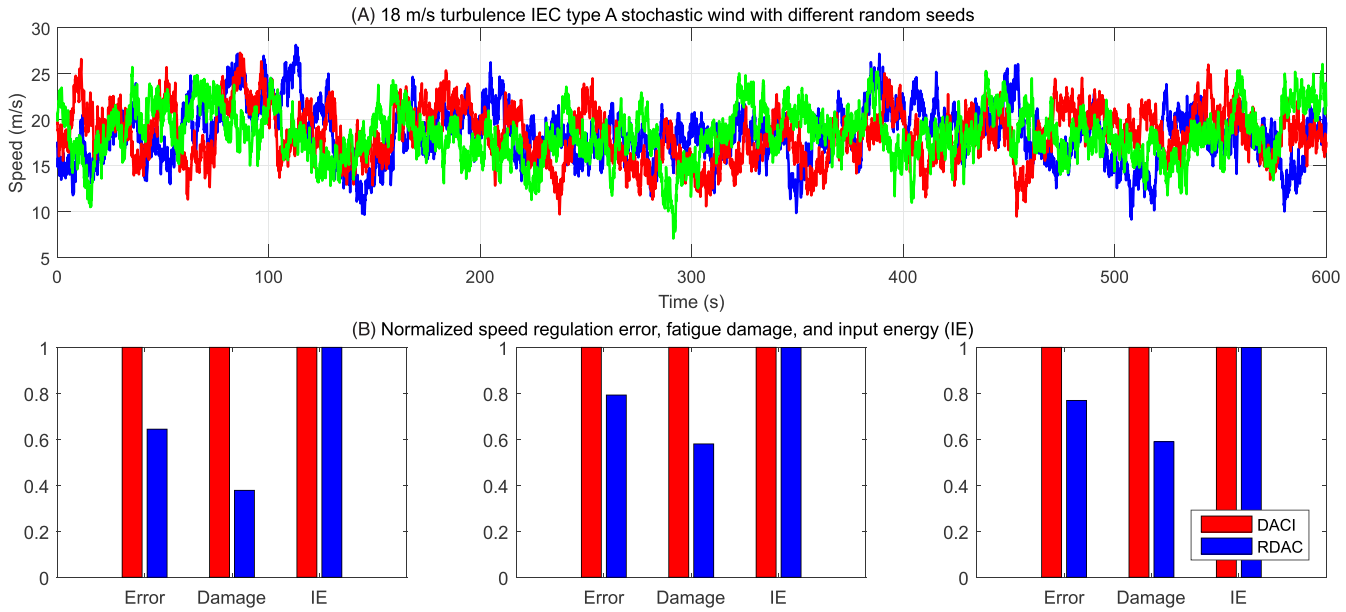

FIGURE 15 Results of stochastic wind profile—10 min simulation with different random seeds (DACI, DAC with integral action; RDAC, Robust DAC) [Colour figure can be viewed at wileyonlinelibrary.com]

algorithm (RFC).[38] The cumulative damage results for different wind profiles are shown in Figure 13b. The normalized mean square rotor speed regulation error and damage of the two controllers are given in Figure 13c. The RDAC approach produces less regulation error and damage than the DACI method for all cases.

To evaluate both speed regulation and structural load reduction and the relationship between those objectives, a covariance distribution diagram measure[19] is used (Figure 14). The generated power (proportional to the rotor speed) and the corresponding structural load (here is tower bending moment) of each controller at a certain point of time are plotted in a single diagram. Speed regulation and structural load reduction performances of each controller are reflected by the standard variations of the related data distribution. With that manner, the dimensions of the covariance ellipse can represent both speed regulation and structural load reduction performances. Lower dimensions mean better control

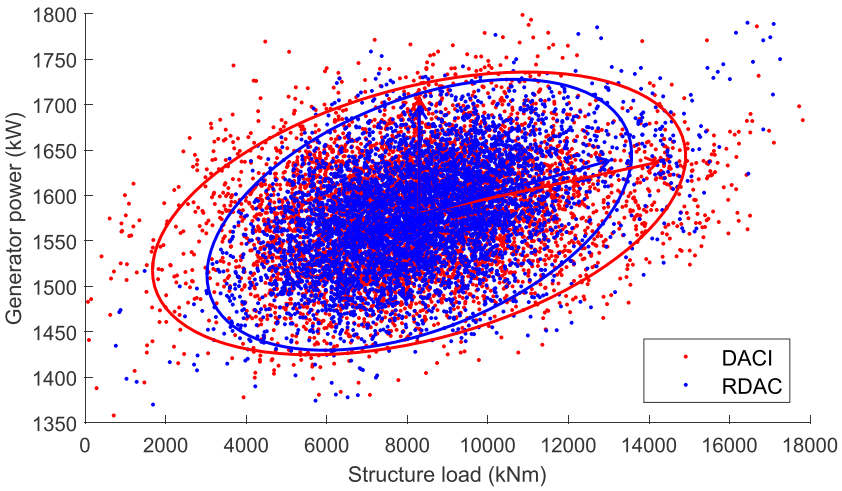

FIGURE 16 Power-load covariance distribution diagram 10 min simulation with different random seeds (DACI, DAC with integral action; RDAC, Robust DAC) [Colour figure can be viewed at wileyonlinelibrary.com]

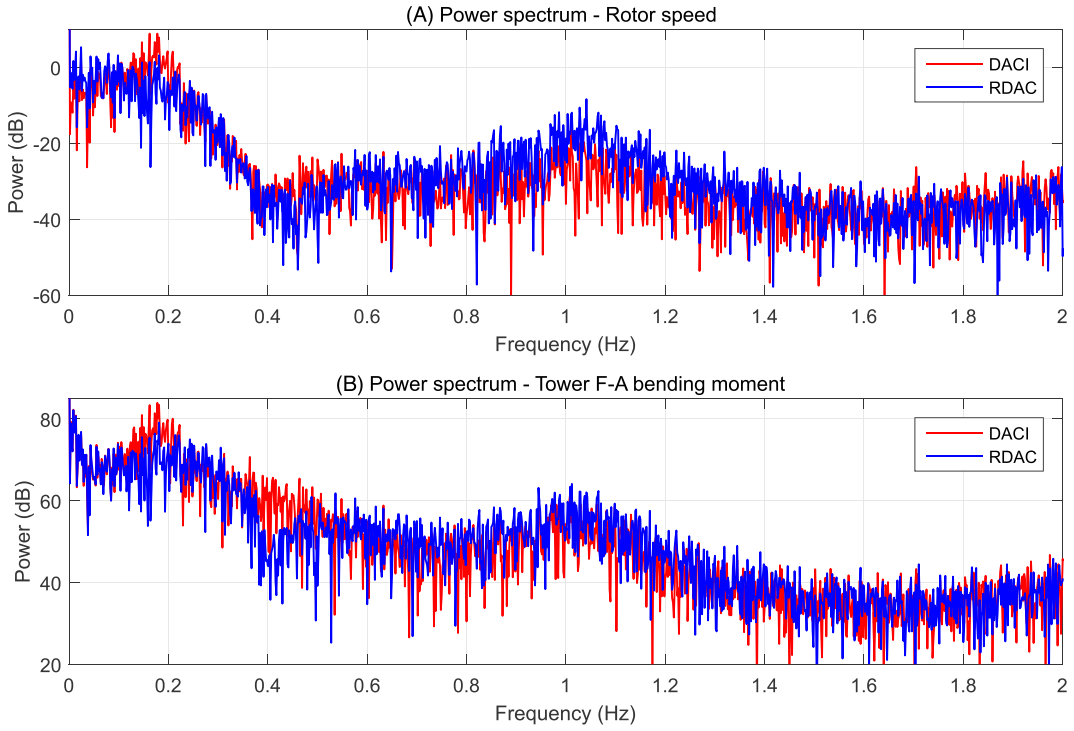

FIGURE 17 Power spectrum analysis (DACI, DAC with integral action; RDAC, Robust DAC) [Colour figure can be viewed at wileyonlinelibrary.com]

performances in speed regulation and structural load reduction, respectively. It can be detected that the covariance ellipse representing the RDAC approach is smaller than that of the DACI controller demonstrating better performances of RDAC for both objectives.

The analysis results for 600 s (10 min) of stochastic wind with different random seeds are shown in Figures 15 and 16. Advantages of the RDAC approach over the DAC approach designed by LQG and Kronecker product (DACI) are clearly shown in the figures with respect to lower speed regulation error and fatigue damage. The blade pitch activities or the input energy are nearly the same for both controllers. From the power spectrum analysis of the rotor speed and tower bending moment responses (Figure 17), it can be observed that the proposed RDAC approach can compress the speed and moment variations in the low-frequency region compared to the DACI approach.

6 | CONCLUSIONS

A new method to design disturbance accommodating control (DAC) system for wind turbine load mitigation control in region 3 is developed. The DAC including disturbance observer, feedback controller, and disturbance rejection controller is considered as a single dynamic controller. The parameters of the dynamic controller are computed by minimizing the mixed-sensitivity H_∞ norm of the closed-loop transfer functions with structure and stability constraints using the non-smooth optimization technique. Integral action is included in the dynamic controller instead of in the generalized plant for zero steady-state tracking error of the rotor speed. Simulation results show that the proposed method is able to regulate the rotor speed without steady-state error despite the presence of the model uncertainties. The proposed RDAC approach has better speed regulation and structural load reduction performances in comparison with the DAC controller designed by the Kronecker product method. The proposed approach also provides high robustness against the imprecise model caused by the use of reduced-order linearized model and unknown wind disturbances.

The proposed RDAC and the baseline DAC controllers are designed at a single operating point. The controller can operate robustly with fixed parameters under a wide range of wind speeds. However, to improve the control performance, gain-scheduling techniques can be employed for several operating points in future work. This might also allow more detailed comparisons which existing classical gain-scheduling methods known from literature. The approach introduced establishes therefore a new baseline approach for robust control integrating load mitigation.

The proposed RDAC approach uses the mix-sensitivity H_∞ norm as a cost function for the optimization problem. The robustness and performance of each output channel can be designed by weight functions for different frequency ranges. The weight functions can be adapted to the actual wind dynamics with related dominating frequencies for a more effective situation-based balance between robustness and performance. The weights also can be chosen depending on the situation-based demands from grid operators.

In this paper, two linear DAC design approaches are compared in region 3. For better evaluation of the new approach, further studies might be required using more realistic conditions in comparison with a well-tuned, gain-scheduled baseline controller with a proper tower damper over the full operating range.

ACKNOWLEDGEMENT

The research reported in this paper is partly supported by the Vietnam International Education Development (VIED) scholarship received by the first author for his Dr.-Ing. study at the Chair of Dynamics and Control, UDE, Germany.

PEER REVIEW

The peer review history for this article is available at https://publons.com/publon/10.1002/we.2663.

DATA AVAILABILITY STATEMENT

The data that support the findings of this study are available from the corresponding author upon reasonable request.

ORCID

M. Hung Do https://orcid.org/0000-0002-8485-4139
Dirk Söffker https://orcid.org/0000-0001-8299-101X

REFERENCES

1. Bossanyi EA. Individual blade pitch control for load reduction. *Wind Energy: An Int J Prog Appl Wind Power Convers Technol*. 2003;6(2):119-128.
2. Johnson CD. Theory of disturbance-accommodating controllers. *Control Dyn Syst*. 1976;12:387-489.
3. Njiri JG, Söffker D. State-of-the-art in wind turbine control: trends and challenges. *Renew Sustain Energy Rev*. 2016;60:377-393.
4. Liu Y, Söffker D. Improvement of optimal high-gain pi-observer design. In: 2009 european control conference (ecc) 2009 European Control Conference (ECC); 2009:4564-4569.
5. Imran RM, Hussain DMAkbar, Soltani M. Dac with lqr control design for pitch regulated variable speed wind turbine. In: 2014 ieee 36th international telecommunications energy conference (intelec) 2014 IEEE 36th International Telecommunications Energy Conference (INTELEC); 2014:1-6. https://doi.org/10.1109/intlec.2014.6972153

6. Imran RM, Hussain DA, Soltani M. DAC to mitigate the effect of periodic disturbances on drive train using collective pitch for variable speed wind turbine. In: 2015 IEEE International Conference on Industrial Technology (ICIT) 2015 IEEE International Conference on Industrial Technology (ICIT); 2015:2588-2593. https://doi.org/10.1109/icit.2015.7125479
7. Girsang IP, Dhupia JS. Collective pitch control of wind turbines using stochastic disturbance accommodating control. *Wind Eng*. 2013;37(5):517-533.
8. Wang N, Wright AD, Johnson KE. Independent blade pitch controller design for a three-bladed turbine using disturbance accommodating control. In: American control conference (ACC), 2016 IEEE American Control Conference (ACC) 2016; 2016:2301-2306. https://doi.org/10.1109/acc.2016.7525261
9. Wang N, Wright AD, Balas MJ. Disturbance accommodating control design for wind turbines using solvability conditions. *J Dyn Syst, Meas, Control*. 2017;139(4):041007.
10. Njiri JG, Söffker D. Multi-objective optimal control of wind turbines for speed regulation and load reduction. In: Asme 2015 dynamic systems and control conference ASME 2015 Dynamic Systems and Control Conference; 2015:V001T05A002-V001T05A002. https://doi.org/10.1115/dscc2015-9787
11. Do MH, Njiri JG, Söffker D. Structural load mitigation control for nonlinear wind turbines with unmodeled dynamics. In: 2018 annual american control conference (acc) IEEE 2018 Annual American Control Conference (ACC); 2018:3466-3471. https://doi.org/10.23919/acc.2018.8431121
12. Gahinet P, Apkarian P. Structured h_∞ synthesis in matlab. *IFAC Proc Vol*. 2011;44(1):1435-1440.
13. Do MH, Söffker D. Robust observer-based load extenuation control for wind turbines. In: 15th international conference on multibody systems, nonlinear dynamics, and control (msndc) ASME 15th International Conference on Multibody Systems, Nonlinear Dynamics, and Control (MSNDC); 2019. https://doi.org/10.1115/detc2019-97645
14. Geyler M, Caselitz P. Robust multivariable pitch control design for load reduction on large wind turbines. *J Solar Energy Eng*. 2008;130(3):031014.
15. De Corcuera AD, Pujana-Arrese A, Ezquerra JM, Segurola E, Landaluze J. h_∞ based control for load mitigation in wind turbines. *Energies*. 2012;5(4):938-967.
16. Fleming P, Wingerden J-W, Wright A. Comparing state-space multivariable controls to multi-siso controls for load reduction of drivetrain-coupled modes on wind turbines through field-testing. In: 50th aiaa aerospace sciences meeting including the new horizons forum and aerospace exposition; 2012:1152.
17. Jonkman JM, Buhl Jr ML. Fast user's guide-updated August 2005. *tech. rep*., National Renewable Energy Laboratory (NREL), Golden, CO.; 2005.
18. Dykes KL, Rinker J. Windpact reference wind turbines. *tech. rep*., National Renewable Energy Lab (NREL), Golden, CO (United States); 2018.
19. Do MH, Njiri JG, Söffker D. Structural load mitigation control for wind turbines: a new performance measure. *Wind Energy*. 2020;23:1085-1098.
20. Wright AD, Fingersh LJ. Advanced control design for wind turbines; part I: control design, implementation, and initial tests. *tech. rep*., National Renewable Energy Lab.(NREL), Golden, CO (United States); 2008.
21. Söffker D, Yu T-J, Müller PC. State estimation of dynamical systems with nonlinearities by using proportional-integral observer. *Int J Syst Sci*. 1995;26(9):1571-1582.
22. Liu Y, Söffker D. Robust control approach for input-output linearizable nonlinear systems using high-gain disturbance observer. *Int J Robust Nonlinear Control*. 2014;24(2):326-339.
23. Davison E. The output control of linear time-invariant multivariable systems with unmeasurable arbitrary disturbances. *IEEE Trans Autom Control*. 1972;17(5):621-630.
24. Gahinet P, Apkarian P. A linear matrix inequality approach to h_∞ control. *Int J Robust Nonlinear Control*. 1994;4(4):421-448.
25. Doyle JC, Glover K, Khargonekar PP, Francis BA. State-space solutions to standard h_2 and h_∞ control problems. *IEEE Trans Autom Control*. 1989;34(8):831-847.
26. Skogestad S, Postlethwaite I. *Multivariable Feedback Control: Analysis and Design*, Vol. 2. New York: Wiley; 2007.
27. Apkarian P, Noll D. The h_∞ control problem is solved. *AerospaceLab J*. 2017;13:1-11.
28. Apkarian P, Noll D. Nonsmooth h_∞ synthesis. *IEEE Trans Autom Control*. 2006;51(1):71-86.
29. Desoer CA, Vidyasagar M. *Feedback Systems: Input-Output Properties*, Vol. 55: Siam; 1975.
30. Boyd S, Balakrishnan V, Kabamba P. A bisection method for computing the h_∞ norm of a transfer matrix and related problems. *Math Control, Sig Syst*. 1989;2(3):207-219.
31. Clarke FH. *Optimization and Nonsmooth Analysis*: Society for Industrial and Applied Mathematics; 1990.
32. Bruinsma NA, Steinbuch M. A fast algorithm to compute the h_∞ of a transfer function matrix. *Syst Control Lett*. 1990;14(4):287-293.
33. IEC. Iec 61400-1: Wind turbines part 1: design requirements. International Electrotechnical Commission; 2005.
34. Wright AD. Modern control design for flexible wind turbines. *tech. rep*., National Renewable Energy Lab.(NREL), Golden, CO (United States); 2004.
35. Jonkman BJ, Buhl Jr ML. Turbsim user's guide. *tech. rep*., National Renewable Energy Lab (NREL), Golden, CO (US); 2009.
36. Schütz W. A history of fatigue. *Eng Fract Mech*. 1996;54(2):263-300. https://doi.org/10.1016/0013-7944(95)00178-6
37. Miner MA. Cumulative damage in fatigue. *J Appl Mech*. 1945;12(3):A159-A164.
38. Matsuishi M, Endo T. Fatigue of metals subjected to varying stress. *Japan Soc Mech Eng, Fukuoka, Japan*. 1968;68(2):37-40.

How to cite this article: Do MH, Söffker D. Wind turbine robust disturbance accommodating control using non-smooth H_∞ optimization. *Wind Energy*. 2021;1–18. https://doi.org/10.1002/we.2663